AERO 520 INTRO. TO AEROSPACE DESIGN

Institute for Aerospace Eng. (Faculty of Engineering)

Winter 2026

Report #1

Preliminary Sizing for Aircraft

Evelyne Jewitt-Dyck: 261087480

Iris Sam Chacko: 261202510

Maverick Hoziel: 261115085

Milka Ininahazwe: 261214360

ABSTRACT

This report presents the preliminary weight and performance sizing for a new aircraft design developed in response to a specific Request for Proposal (RFP). The objective was to translate the RFP's mission requirements including payload, range, and cruise speed into a viable aircraft configuration. Using Advanced Aircraft Analysis (AAA) V5.1 by DARcorporation, an iterative sizing methodology was employed to determine the Maximum Take-off Weight (MTOW) and Empty Weight (W_E). The analysis utilized mission fuel fractions and Breguet's equations to ensure the design satisfies all phases of the mission profile, from takeoff to landing with required reserves. Furthermore, a performance matching analysis was conducted to establish the optimal thrust-to-weight ratio (T/W) and wing loading (W/S) required to meet the specific performance constraints outlined in the RFP. The resulting design point provides a converged, physics-based foundation for the subsequent preliminary configuration and detailed design phases.

TABLE OF CONTENTS

TABLE OF TABLES

TABLE OF FIGURES

1. RFP SUMMARY

This RFP (Request for Proposal) requests for the conceptual design of a next generation ultra-premium long-range business jet intended to compete with aircrafts like the Bombardier Global 7500 or Gulfstream G650/700, emphasizing on luxury cabins and challenging performance targets. The RFP highlights the mandatory requirements as well as the tradable ones. The mandatory requirements are [1]:

General

- Must takeoff and land from standard airport runways
- Must take off and land on 6000ft runway, sea-level standard day, grooved concrete, dry runway
- 8000NM of range
- Minimum cruise speed of Mach 0.85
- Capable of VFR and IVR operations
- Capable of flight in known icing conditions
- Must meet FAA 14 CFR Part 25 requirements

Interior

- Seating for 8 passengers (60in pitch and 22in seat width)
- Seating for 1 flight attendant in passenger cabin
- Queen-size bed (60in by 80in) in private room
- Two lavatories, including one handicap-accessible with a hot-water shower and 30 minutes of water capabilities
- One galley sized for the design range mission and accessible by flight attendant
- Flight deck for two pilots, plus one passenger-accessible jump seat
- Infrastructures for Wi-Fi and satellite TV
- Cabin pressurization equivalent to 6000ft cabin altitude at max service ceiling
- Maintain more or equal 30% of baggage area at 45 Fahrenheit on a 100 Fahrenheit day at sea level
- Assuming 215lbs per passenger and crew member with 50lbs baggage
- 8 cubic feet of baggage per passenger

The tradable requirements are [1]:

- Target cruise speed of Mach 0.92
- Maximum dive speed to not exceed Mach 0.995
- Passenger seats may be lay-flat reclinable
- Optional crew rest area, based on crew requirements

The aircraft concept is designed to satisfy the mandatory requirements, while using the tradable requirements as performance and comfort stretch targets to increase appeal and outselling competitors.

2. WEIGHT SIZING

The weight sizing phase of the preliminary design process was executed to establish the fundamental weight limits of the aircraft, specifically the Maximum Takeoff Weight (MTOW) and the Manufacturer's Weight Empty (MWE). This analysis was conducted using Advanced Aircraft Analysis (AAA) V5.1 by DAR corporation, which facilitates an iterative regression-based approach. The process began by defining the mission payload and crew requirements, followed by the development of a specific mission profile to estimate fuel consumption. By applying fuel weight fractions and Breguet's equations for range and endurance, the software iteratively calculated the fuel requirements for each flight phase—including warmup, climb, cruise, and loiter. This methodology ensures that the aircraft is sized appropriately to meet all performance objectives before proceeding to configuration design. The following sections detail the specific mission profile, the fuel fraction assumptions, and the resulting weight iterations.

2.1. Mission Profile Description

The mission profile will consist of eight (8) segments:

1. Warm up
2. Taxi
3. Takeoff
4. Climb

5. Cruise
6. Descent
7. Loiter
8. Land & Taxi

We believe that this sequence of flight phase is the one that will be the most often executed by the owner of our aircraft. We have decided to climb to cruising altitude in one step, and not in multiple steps to get to cruising altitude and speed as fast as possible to be able to get to destination as fast as possible since time is extremely important for our wealthy owners. Also, the loiter phase is planned to be after the descent; to simulate the event that ATC (Air Traffic Control) communicates with the pilot that landing will have to be delayed. After that, the aircraft lands and taxis to its destination. The schematic for the mission is given below.

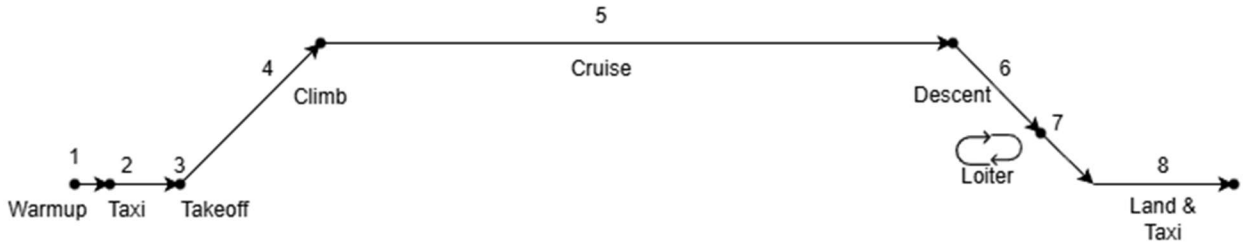

Figure 1: Mission profile schematic

The mission fuel fraction is calculated below for each segment in the mission phase

Table 1: Weight and Fuel Fraction

Segment	**Begin Weight (W_b) lb**	**Fuel Begin Weight (W_{Fbegin}) lb**	**Fuel Fraction (M_{ff})**	**Fuel used (ΔW_{Fused}) lb**
1	115158.2	48049.0	0.9900	1151.6
2	114006.6	46897.4	0.9950	570.0
3	113436.6	46327.4	0.9950	567.2
4	112869	45760.2	0.9864	1531.4
5	111338.0	44228.8	0.6714	36580.6
6	74757.4	7646.2	0.9900	747.6

7	74009.8	6900.6	0.9736	1956.1
8	72053.7	4944.5	0.9920	576.4

2.2. Weight Estimations

The weight estimation was conducted to determine the aircraft's Maximum Take-off Weight (W_{TO}) and Empty Weight (W_E). The procedure began by establishing the mission payload and crew requirements as defined by the RFP (McGill University, 2026). Using AAA software, we input a preliminary guess for the take-off weight based on similar existing aircraft. The software then calculated the mission fuel weight (W_F) by analyzing individual fuel fractions for each flight phase from warmup and takeoff to cruise and landing utilizing Breguet's range and endurance equations. Simultaneously, the allowable empty weight was determined through a regression analysis of historical data using constants (A and B) specific to the aircraft's category. The assumptions and calculations are given in the following sections.

2.2.1. Aerodynamic and propulsion efficiency (SFC, L/D) Assumptions

The preliminary sizing for this aircraft is based on a high-bypass ratio turbofan configuration. This architecture was selected to optimize efficiency during the Mach 0.85 cruise segment, which is a critical driver for achieving the mandated 8,000 nautical mile range. (McGill University, 2026) By accelerating a large mass of air at a lower velocity relative to the core exhaust, the high-bypass design provides the superior energy conversion necessary for long-range missions while ensuring compliance with the 2035 Entry-into-Service (EIS) target. Propeller efficiency (η_p) is not applicable to this design, as the aircraft utilizes turbofans rather than a propeller-driven system.

For the weight sizing process, the thrust specific fuel consumption (c_j) during cruise is assumed to be 0.9 lb/lb/hr, which aligns with the suggested values for business jets found in Figure 2 found below. The value $c_j = 0.9$ lb/lb/hr was selected conservatively, as it corresponds to the highest expected fuel consumption within the typical range, preventing the design from relying on optimistic efficiency assumptions. For loiter, $c_j = 0.5$lb/lb/hr was assumed, representing the midpoint of the 0.4 to 0.6 range. Because loiter has a smaller impact on total fuel burn than cruise, and cruise was treated conservatively, the average value was chosen to maintain a

balanced overall estimate. These efficiency parameters are fundamental to the mission fuel fraction calculations, as the cruise segment typically represents the largest fuel burn of the mission profile.

The aerodynamic configuration uses a high-aspect-ratio wing equipped with advanced supercritical airfoils to maximize the lift-to-drag (L/D) ratio while mitigating wave drag at high subsonic speeds. The lift-to-drag ratio assumed for the climb segment was selected to be slightly lower than the cruise value, since climb typically occurs at a higher angle of attack. At elevated angles of attack, drag increases more rapidly than lift, which leads to a reduction in the lift-to-drag ratio [3]. Therefore, a value of 16 was adopted for the climb segment. A baseline cruiseL/D of 18.0 is established to satisfy the long-range objectives efficiently. The value of 18 was selected based on class discussion indicating that modern business jets typically achieve lift-to-drag ratios in the range of 18 to 20, which is significantly higher than the 10 to 12 range illustrated in Figure 2. For the loiter segment, a maximum aerodynamic efficiency $(L/D)_{max}$ of 14.0 was assumed based on the suggested values for business aircraft shown in Figure 2. Although class discussion indicated that modern aircraft may achieve higher L/D ratios, a conservative value of 14 was retained for this analysis.

Table 2.2 Suggested Values For L/D, c_j, η_p,And For c_p For Several Mission Phases

	Cruise				Loiter			
	L/D	c_j	c_p	η_p	L/D	c_j	c_p	η_p
Mission		lbs/lbs/hr	lbs/hp/hr			lbs/lbs/hr	lbs/hp/hr	
Phase No.(See Fig.2.1)		5				6		
Airplane Type								
1. Homebuilt	8-10*		0.6-0.8	0.7	10-12		0.5-0.7	0.6
2. Single Engine	8-10		0.5-0.7	0.8	10-12		0.5-0.7	0.7
3. Twin Engine	8-10		0.5-0.7	0.82	9-11		0.5-0.7	0.72
4. Agricultural	5-7		0.5-0.7	0.82	8-10		0.5-0.7	0.72
5. Business Jets	10-12	0.5-0.9			12-14	0.4-0.6		
6. Regional TBP's	11-13		0.4-0.6	0.85	14-16		0.5-0.7	0.77
7. Transport Jets	13-15	0.5-0.9			14-18	0.4-0.6		
8. Military Trainers	8-10	0.5-1.0	0.4-0.6	0.82	10-14	0.4-0.6	0.5-0.7	0.77
9. Fighters	4-7	0.6-1.4	0.5-0.7	0.82	6-9	0.6-0.8	0.5-0.7	0.77
10. Mil.Patrol, Bomb, Transport	13-15	0.5-0.9	0.4-0.7	0.82	14-18	0.4-0.6	0.5-0.7	0.77
11. Flying Boats, Amphibious, Float Airplanes	10-12	0.5-0.9	0.5-0.7	0.82	13-15	0.4-0.6	0.5-0.7	0.77
12. Supersonic Cruise	4-6	0.7-1.5			7-9	0.6-0.8		

Figure 2: Suggested values for L/D, c_j, c_p, n_p for Cruise and Loiter [2]

2.2.2. Estimation of Empty weight – Regression analysis

The estimation of the aircraft's Empty Weight (W_E) was performed using a statistical regression analysis based on historical data from similar aircraft categories. This methodology utilizes the relationship below:

$$log_{10} W_E = \frac{log_{10} W_{T0} - A}{B}$$

where A and B are regression constants specific to the aircraft type, such as Business Jets or Transport Jets. By applying these constants within the Advanced Aircraft Analysis (AAA) software, we established a trend line that defines the "allowable" empty weight for a given Maximum Take-off Weight (W_{TO}).

The following values for A and B were taken from the Standard Values for business class jets (Roskam, 1997), displayed in Figure 3 below

A = 0.2678 B = 0.9979

Table 2.15 Regression Line Constants A and B of Equation (2.16)

Airplane Type	A	B
1. Homebuilts		
Pers. fun and transportation	0.3411	0.9519
Scaled Fighters	0.5542	0.8654
Composites	0.8222	0.8050
2. Single Engine Propeller Driven	-0.1440	1.1162
3. Twin Engine		
Propeller Driven	0.0966	1.0298
Composites	0.1130	1.0403
4. Agricultural	-0.4398	1.1946
5. Business Jets	0.2678	0.9979
6. Regional TBP	0.3774	0.9647
7. Transport Jets	0.0833	1.0383
8. Military Trainers		
Jets	0.6632	0.8640
Turboprops	-1.4041	1.4660
Turboprops without No.2	0.1677	0.9978
Piston/Props	0.5627	0.8761
9. Fighters		
Jets(+ ext.load)	0.5091	0.9505
Jets(clean)	0.1362	1.0116
Turboprops(+ ext.load)	0.2705	0.9830
10. Mil. Patrol, Bomb and Transport		
Jets	-0.2009	1.1037
Turboprops	-0.4179	1.1446
11. Flying Boats, Amphibious and Float Airplanes	0.1703	1.0083
12. Supersonic Cruise	0.4221	0.9876

Figure 3: Regression Line constants A and B [2]

Furthermore, as previously discussed, regression analysis was used to estimate the aircraft's takeoff and empty weights. The resulting design point is shown in Figure 4.

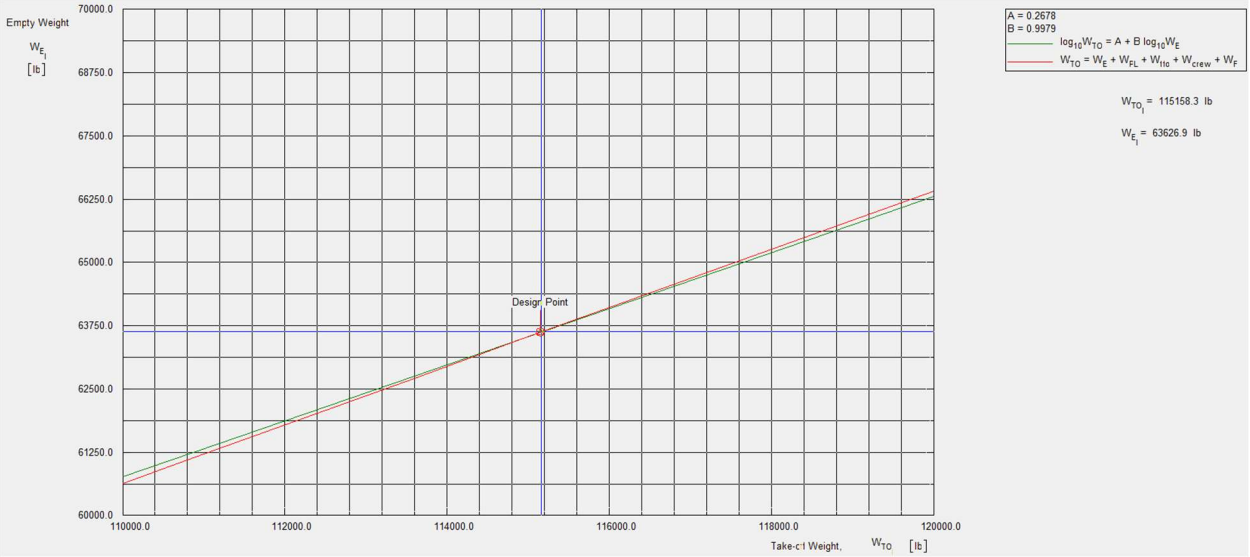

Figure 4: Empty and takeoff weight design point

Note that the takeoff and empty weight values shown in Figure 4 do not exactly match those provided by AAA. This discrepancy is due to the limited precision of the cursor when selecting the design point. Nevertheless, the values shown provide a close approximation of the true results.

2.2.3. Final Design Weights (Takeoff weight, empty weight, fuel weight, payload weight, trapped fuel & oil weight)

The table below represents the finalized mass properties of the aircraft, which will serve as the baseline for all subsequent aerodynamic and stability analyses.

Table 2: Final Design Weights

Final Design Weights	**Weight (lb)**
Takeoff Weight (max) W_{TOI}	115158.18
Empty Weight W_E	63618.38
Fuel Weight W_F	48049.00
Payload Weight W_{pl}	2270.00
Trapped fuel & oil weight W_{tfo}	575.79

2.3. Sensitivity Study

In preliminary aircraft design, a sensitivity study is essential to evaluate how fluctuations in mission requirements or aerodynamic parameters affect the overall size of the vehicle. Since the

design process involves a continuous series of compromises, these studies identify the growth factors that dictate how much the Takeoff weight must increase to maintain performance if a design variable changes.

For our project, we utilized the partial derivatives within the AAA software to quantify these impacts. This analysis allowed us to determine the weight penalty associated with increases in payload (W_{pl}), or range (R), as well as the potential weight savings gained from improving the lift-to-drag ratio (L/D) or the engine efficiency (c_{jet}). By understanding these sensitivities, we were able to validate the robustness of our sizing and identify the most critical areas for potential research and development to optimize the final aircraft weight.

Table 3: Sensitivity Table

Parameters	**Sensitivity Climb**	**Sensitivity Cruise**	**Sensitivity Loiter**
SFC	49415.88	2593587.24	174408.99
L/D	-2779.60	-72044.10	-6228.90
Range	NA	170.60	NA
Endurance	183129.40	NA	116272.70
Payload Weight	41.41		
Empty Weight	1.81		

Interpretation of the sensitivities to all the parameters identified in the sensitivity table

- $\frac{\partial W_{TO}}{\partial C_j}$ = 49415.88 (climb), 2593587.24 (cruise), 174408.99 (loiter).

  These sensitivities quantify how strongly the aircraft takeoff weight W_{TO} responds to changes in the fuel consumption parameter C_j within each flight segment. Here, C_j is defined in units of (lb/hr)/lb, meaning it represents the fuel burn rate per unit aircraft weight. For example, during the climb segment, an increase of 1 C_j implies reduced propulsion efficiency, which increases the fuel required to complete the mission and therefore increases the sized takeoff weight W_{TO} by 49415.88. The same interpretation applies to the cruise and loiter segments, with cruise showing the largest impact on W_{TO}, followed by loiter, and then climb.

- $\frac{\partial W_{TO}}{\partial L/D}$ = -2779.6 (climb), -72044.1 (cruise), -6228.9 (loiter)

  These sensitivities quantify how strongly the aircraft takeoff weight W_{TO} responds to changes in the lift-to-drag ratio (L/D) within each flight segment. For example, during the climb segment, an increase of 1 in (L/D) decreases the required takeoff weight by approximately 2779.6 lb. The same interpretation applies to the cruise and loiter segments, with the negative sign indicating that improving aerodynamic efficiency reduces the fuel required and therefore reduces W_{TO}.

- $\frac{\partial W_{TO}}{\partial R}$ = 170.6 (cruise)

  This sensitivity quantifies how strongly the aircraft takeoff weight W_{TO} responds to changes in the required range. In this case, increasing the range by 1 NM increases the required takeoff weight by approximately 170.6 lb. This increase is primarily driven by the additional fuel required to achieve the longer mission distance, which results in a higher overall takeoff weight.

- $\frac{\partial W_{TO}}{\partial E}$ = 183129.4 (climb), 116272.7 (loiter)

  These sensitivities quantify how strongly the aircraft takeoff weight W_{TO} responds to changes in endurance E, where E is measured in hours. In this case, increasing endurance by 1 hour increases the required takeoff weight by approximately 183129.4 lb for the climb segment and 116272.7 lb for the loiter segment. This increase is primarily driven by the additional fuel required to remain airborne longer, which raises the overall takeoff weight.

- $\frac{\partial W_{TO}}{\partial W_{pl}}$ = 41.41

  This sensitivity quantifies how strongly the aircraft takeoff weight W_{TO} responds to changes in payload weight W_{pl}. In this case, increasing the payload by 1 lb increases the required takeoff weight by approximately 41.41 lb. This amplification occurs because

a higher payload increases the total weight that must be carried, which typically drives additional fuel requirements and cascades into a larger sized takeoff weight

- $\frac{\partial W_{TO}}{\partial W_E} = 1.81$

  This sensitivity quantifies how strongly the aircraft takeoff weight W_{TO} responds to changes in empty weight W_E. In this case, increasing the empty weight by 1 lb increases the required takeoff weight by approximately 1.81 lb. This occurs because a higher structural weight increases the baseline aircraft weight, which in turn typically requires additional fuel and leads to a higher size takeoff weight.

3. PERFORMANCE SIZING

Following the initial weight estimation, performance sizing was conducted to determine the required thrust-to-weight ratio (T/W) and wing loading (W/S) necessary to satisfy the mission's performance constraints. This process involved evaluating the aircraft against several critical design requirements, including stall speed, takeoff distance, climb gradients, and maximum cruise speed. By utilizing AAA Software, these constraints were mapped onto a matching plot to identify the "valid design space" the region where all regulatory and mission-specific performance criteria are met. This sizing ensures that the aircraft possesses sufficient wing area for lift and enough power or thrust for all flight regimes, from low-speed landing maneuvers to high-altitude cruise. The resulting design point selected from this analysis serves as the foundation for the subsequent preliminary configuration and geometry definition.

3.1. Drag Calculations

3.1.1. Equivalent skin friction coefficient

The skin friction coefficient (C_f) is a dimensionless parameter used in aerodynamics to quantify the friction drag exerted on an aircraft's surface as air flows over it. It represents the ratio of the shear stress at the wall to the dynamic pressure of the free-stream flow**.** The skin friction coefficient used in the design of the aircraft was 0.003, as shown in Figure 5.

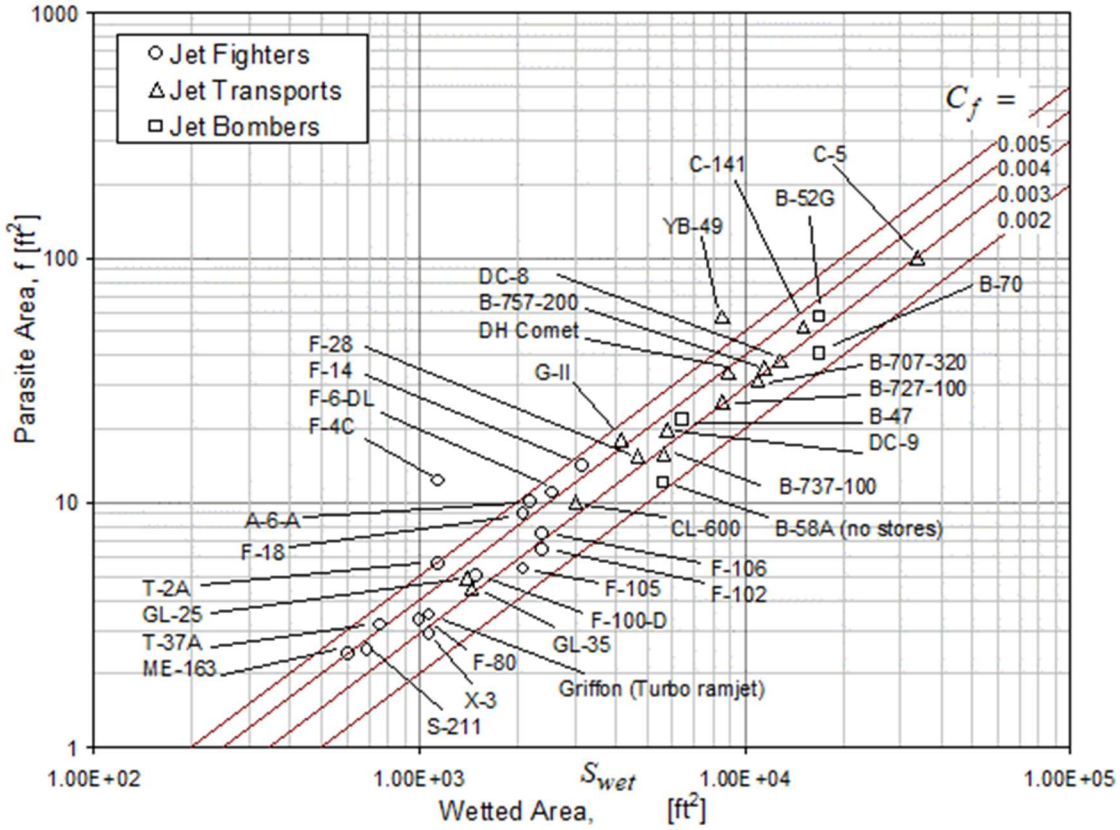

Figure 5: f vs S_wet plot [2]

The value of 0.003 was chosen from the $C_f = 0.003$ line intersecting the Boeing 727-100 and was adopted based on in-class discussion and recommendations.

3.1.2. Regression line constants (a & b) for "f vs Swet" plot

The regression line constants a and b were obtained from Figure 6, which correlates skin friction coefficient values with their corresponding a and b parameters. Based on the selected C_f, values of a=−2.5229 and b=1.0 were chosen. These values, along with f and S_{wet}, were then substituted into the equation shown below.

$$log_{10} f = \text{a} + \text{b}\ log_{10} S_{Wet}$$

$f = Equivalent\ Parasite\ Area = 17.17\ \text{ft}^2$

$S_{wet} = Wetted\ Area = 5722.23\text{ft}^2$

$$log_{10} 17.17 = -2.5529 + 1 * log_{10} 5722.23$$

$$1.23 = 1.23$$

■

Note that the values of f and S_{wet} were obtained as outputs from the AAA software, shown in Figure 7

Table 3.4 Correlation Coefficients for Parasite Area Versus Wetted Area (Eqn.(3.21))

Equivalent Skin Friction Coefficient, c_f	a	b
0.0090	-2.0458	1.0000
0.0080	-2.0969	1.0000
0.0070	-2.1549	1.0000
0.0060	-2.2218	1.0000
0.0050	-2.3010	1.0000
0.0040	-2.3979	1.0000
0.0030	-2.5229	1.0000
0.0020	-2.6990	1.0000

Figure 6: Correlation coefficients for Parasite area versus wetted area [2]

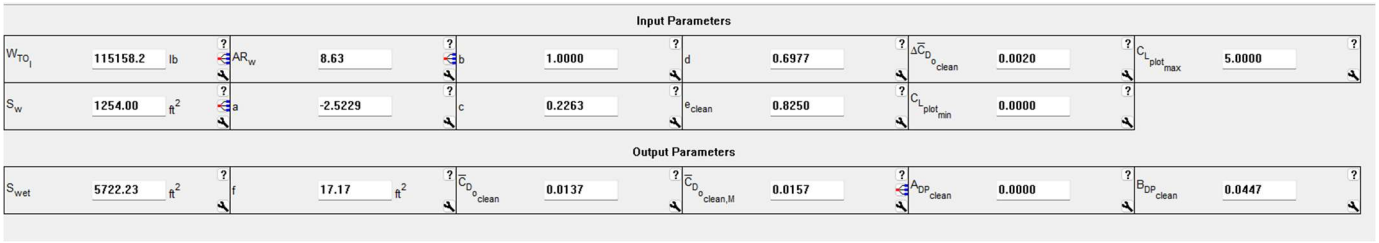

Figure 7: Output parameters of class 1 clean aircraft drag polar

3.1.3. Regression line constants (c & d) for " WTO vs Swet" plot

The regression line constants c & d can be found in in Figure 8 next to the “Business Jet” category.

Table 3.5 Regression Line Coefficients for Take-off Weight Versus Wetted Area (Eqn.(3.22))

Airplane Type	c	d
1. Homebuilts	1.2362	0.4319
2. Single Engine Propeller Driven	1.0892	0.5147
3. Twin Engine Propeller Driven	0.8635	0.5632
4. Agricultural	1.0447	0.5326
5. Business Jets	0.2263	0.6977
6. Regional Turboprops	-0.0866	0.8099
7. Transport Jets	0.0199	0.7531
8. Military Trainers*	0.8565	0.5423
9. Fighters*	-0.1289	0.7506
10. Mil. Patrol, Bomb and Transport	0.1628	0.7316
11. Flying Boats, Amph. and Float	0.6295	0.6708
12. Supersonic Cruise Airplanes	-1.1868	0.9609

* For these airplanes, wetted areas were correlated with 'clean', maximum take-off weights. No stores were accounted for.

Figure 8: Regression line coefficients for takeoff weight versus wetted area [2]

As shown in the figure above, the values of c and d are 0.2263 and 0.6977, respectively. Furthermore, following a similar approach used for a and b, a sanity check was performed to validate these values using the equation below.

$$log_{10} S_{Wet} = c + \mathrm{d}\, log_{10} W_{TO}$$

$$log_{10}(5722.23) = 0.2263 + 0.6977 * log_{10}(115158.18)$$

$$3.76 = 3.76$$

■

3.1.4. Assumptions on Oswald's efficiency factor for Takeoff, Landing and clean configurations

In aircraft design, the Oswald efficiency factor (e) is a correction factor used to account for the increase in drag over an ideal wing as the lift increases. For our design we have taken the following values displayed in Table 4.

Table 4: Oswald's Efficiency Table

Oswald's Efficiency Factor	Value
e_{TO}	0.7800
e_{L}	0.7300
e_{clean}	0.8250

The selected Oswald efficiency factor values were chosen to fall near the midpoint of the ranges provided by the AAA software for each flight configuration shown in Figure 9. Since the design is at a preliminary stage, using representative mid-range values provides a balanced estimate that avoids overly optimistic or pessimistic aerodynamic performance assumptions.

Take-off Oswald Efficiency Factor

Configuration	e
Clean	0.80 - 0.85
Take-off Flaps	0.75 - 0.80
Landing Flaps	0.70 - 0.75
Landing Gear	No Effect

(a)

Landing Oswald Efficiency Factor

Configuration	e
Clean	0.80 - 0.85
Take-off Flaps	0.75 - 0.80
Landing Flaps	0.70 - 0.75
Landing Gear	No Effect

(b)

Oswald Efficiency Factor in the Clean Configuration

Configuration	e
Clean	0.80 - 0.85
Take-off Flaps	0.75 - 0.80
Landing Flaps	0.70 - 0.75
Landing Gear	No Effect

(c)

Figure 9: Different Oswald's Efficiency factors for different flight segments, (a) Takeoff, (b) Landing, and (c) Clean

3.1.5. ΔC_{D0} for flaps and gear

Before presenting the values of the zero-lift drag coefficient (C_{D0}), it is important to first discuss the selected wing aspect ratio, as it serves as a key input parameter in the AAA software's calculation of C_{D0}. The wingspan (b_w) and wing area (S_w) used in this design are 104 ft and 1254 ft², respectively. These values result in a wing aspect ratio of:

$$A_w = \frac{(b_w)^2}{S_w} = 8.63$$

This value was not chosen arbitrarily. Table 5 presents the wing aspect ratios, maximum speeds, and ranges of several modern business jets, providing a comparative basis for selecting an aspect ratio that aligns with the mission requirements of the RFP.

Table 5: Wing aspect ratios for different Business jets

Aircraft	Wingspan (ft)	Wing area (ft^2)	Wing aspect ratio	Range (NM)	Max speed
Gulfstream G650	99.6[4]	1283[5]	7.73[6]	7000[4]	Mach 0.925[4]
Gulfstream G700	103[7]	1283*	8.27[6]	7750[8]	Mach 0.935[7]
Bombardier Global 7500	104[8]	1254[8]	8.63[6]	7700[8]	Mach 0.925[8]
Bombardier Global Express	94[9]	1021[9]	8.65[6]	6000[9]	Mach 0.89[9]
Cessna Citation X+	69.2[10]	527[11]	9.08[6]	3408[10]	Mach 0.935[10]
Dassault Falcon 8X	86.3[12]	761[12]	9.78[6]	6450[12]	Mach 0.9[12]
Gulfstream G550	93.5[13]	1137[13]	7.69[6]	6750[13]	Mach 0.885[13]

**Value not found, assumed from G650*

The decision to adopt the wing aspect ratio of the Bombardier Global 7500 was based on a comparison of aircraft with mission profiles similar to those outlined in the RFP. As shown in Table 5, long-range, high-speed business jets such as the Gulfstream G650, Gulfstream G700, Bombardier Global 7500, and Global Express exhibit aspect ratios ranging from approximately 7.73 to 8.65. Since these aircraft closely match the range and cruise performance targets of the proposed design, this range was considered an appropriate reference.

Additionally, other high-speed aircraft listed in the table, such as the Cessna Citation X+ and Dassault Falcon 8X, feature higher aspect ratios exceeding 9, suggesting that increased aspect ratio can be advantageous for cruise efficiency. However, these aircraft generally serve different mission profiles or operate under different design constraints compared to the RFP requirements.

Based on this analysis, the design space was narrowed to the higher end of the 7.73 to 8.65 aspect ratio range. This resulted in two primary reference candidates: the Global 7500 and the Global Express. The Global 7500 was ultimately selected because its range and cruise speed

more closely align with the performance objectives defined in the RFP, making it a more representative benchmark for the proposed aircraft design.

Now, with the wing aspect ratio, we were able to find various C_{D0} and ΔCD_0 using the AAA software. All the values are present in table 6.

Table 6: C_{D0} and ΔC_{D0} for various configurations

Configuration	CD_{0clean}	$CD_{0,configuration}$	$\Delta CD_{0,configuration}$
Clean	0.0137	$CD_{0clean,M} = 0.0157$	$\Delta CD_{0clean} = 0.0020$
Takeoff flaps, gear up	0.0137	$CD_{0Toup} = 0.0287$	$\Delta CD_{0Toup} = 0.0150$
Takeoff flaps, gear down	0.0137	$CD_{0Todwn} = 0.0417$	
Landing flaps, gear up	0.0137	$CD_{0Lup} = 0.0787$	$\Delta CD_{0Lup} = 0.0650$
Landing flaps, gear down	0.0137	$CD_{0Ldwn} = 0.1037$	$\Delta CD_{0Ldwn} = 0.0900$

Additionally, the data shown in Figure 9 validate the values reported in Table 6.

Table 3.6 First Estimates for ΔC_{D_o} and 'e'

With Flaps and Gear Down

Configuration	ΔC_{D_o}	e
Clean	0	0.80 - 0.85
Take-off flaps	0.010 - 0.020	0.75 - 0.80
Landing Flaps	0.055 - 0.075	0.70 - 0.75
Landing Gear	0.015 - 0.025	no effect

Figure 9: First Estimates for ΔC_{D0} & e [2]

3.1.7. Drag polar in clean, takeoff and landing configurations

The drag polar is the total equation that describes the relationship between lift and drag for your aircraft. It is expressed as:

$$C_D = C_{D0} + \frac{C_L^2}{\pi . AR . e}$$

Where C_{D0} is Zero lift Drag Coefficient. It represents the drag the aircraft produces when it is generating zero lift.

The calculated values for the drag polar and C_{D0} are given in Table 8 below:

Table 7: Drag polar and C_{D0}

	Clean	Takeoff, gear down	Takeoff, gear up	Landing, gear down	Landing, gear up
Drag polar	$C_D = 0.0157 + 0.0447C_L^2$	$C_D = 0.0.0417 + 0.0473C_L^2$	$C_D = 0.0287 + 0.0473C_L^2$	$C_D = 0.1037 + 0.0506C_L^2$	$C_D = 0.0787 + C_L^2$
C_{D0}	0.0157	0.0417	0.0287	0.1037	0.0787

3.1.8. Assumptions in $C_{L_{max}}$ in Takeoff, landing and clean configurations

In order to move from a theoretical weight to an actual flying machine, we established how much lift the wings could realistically generate. These $C_{L_{max}}$ values are essentially the performance ceiling for the wings; if they are underestimated, the plane becomes too heavy to take off, but if we are too optimistic, the plane will not be able to land safely on a standard runway. Using the data for business jets found in Figure 10, we selected values that specifically prioritize the RFP's requirements,

We assumed a $C_{L_{max}}$ of 1.7 for clean, a $C_{L_{max_{TO}}}$ of 2.10 for takeoff and a $C_{L_{max_L}}$ of 2.50 for landing. These values are representative of modern high-performance wing designs equipped with advanced high-lift devices. The selected coefficients were guided by the range of values presented in Figure 10, from which values near the upper end of the spectrum were chosen while remaining within realistic bounds.

This decision reflects the assumption that the aircraft will incorporate advanced aerodynamic technologies anticipated to be available by 2035. As a result, slightly optimistic yet still credible lift performance values were considered appropriate for this preliminary design analysis.

Table 3.1 Typical Values For Maximum Lift Coefficient

Airplane Type	$C_{L_{max}}$	$C_{L_{max_{TO}}}$	$C_{L_{max_L}}$
1. Homebuilts	1.2 - 1.8	1.2 - 1.8	1.2 - 2.0*
2. Single Engine Propeller Driven	1.3 - 1.9	1.3 - 1.9	1.6 - 2.3
3. Twin Engine Propeller Driven	1.2 - 1.8	1.4 - 2.0	1.6 - 2.5
4. Agricultural	1.3 - 1.9	1.3 - 1.9	1.3 - 1.9
5. Business Jets	1.4 - 1.8	1.6 - 2.2	1.6 - 2.6
6. Regional TBP	1.5 - 1.9	1.7 - 2.1	1.9 - 3.3
7. Transport Jets	1.2 - 1.8	1.6 - 2.2	1.8 - 2.8
8. Military Trainers	1.2 - 1.8	1.4 - 2.0	1.6 - 2.2
9. Fighters	1.2 - 1.8	1.4 - 2.0	1.6 - 2.6
10. Mil. Patrol, Bomb and Transports	1.2 - 1.8	1.6 - 2.2	1.8 - 3.0
11. Flying Boats, Amphibious and Float Airplanes	1.2 - 1.8	1.6 - 2.2	1.8 - 3.4
12. Supersonic Cruise Airplanes	1.2 - 1.8	1.6 - 2.0	1.8 - 2.2

Figure 10: Typical values for $C_{L_{max}}$ [2]

Moreover, climb gradients requirements CGR for FAR 25 were checked and our aircraft was able to achieve the required CGRs for FAR25 for a two-engine plane, as depicted in Figure 11.

$F_{MaxCont}$	0.900	$C_{L_{max_{TO}}}$	2.100	W_L/W_{TO}	0.635	$\overline{C}_{D_{0_{TO\_up}}}$	0.0287	$B_{DP_{TO\_down}}$	0.0473	$\Delta\overline{C}_{D_{0_A}}$	0.0035
F_{8sec}	1.000	$C_{L_{max_A}}$	2.300	$\overline{C}_{D_{0_{clean,M}}}$	0.0157	$B_{DP_{TO\_up}}$	0.0473	$\overline{C}_{D_{0_{L\_down}}}$	0.1037	$C_{D_{wm}}$	0.0035
$C_{L_{max_{clean}}}$	1.700	$C_{L_{max_L}}$	2.500	$B_{DP_{clean}}$	0.0447	$\overline{C}_{D_{0_{TO\_down}}}$	0.0417	$B_{DP_{L\_down}}$	0.0506	CGR	FAR 25
Output Parameters											
$CGR_{25.111}$	0.012	$CGR_{25.121_T}$	0.000	$CGR_{25.121_{SS}}$	0.024	$CGR_{25.121_{ER}}$	0.012	$CGR_{25.121_L}$	0.021	$CGR_{25.119}$	0.032

Figure 11: Far 25 Climb gradients requirements

3.2. Plots

The aerodynamic efficiency of the design is captured through a series of drag polars which illustrate how the aircraft's physical state transitions to meet the specific demands of each flight phase. A comparative study of the drag coefficient (C_D), lift-to-drag ratio (C_L/C_D), and endurance ($C_L^{0.5}/C_D$) curves across Figures 12,13, and 14 reveals the aerodynamic evolution of the aircraft as it transitions from the high-lift requirements of departure to high-speed cruise, and finally, to low-speed landing.

In the takeoff configuration (Figure 12), the deployment of takeoff flaps and gear results in a zero-lift drag of 0.0417. In this state, the peak of the C_L/C_D curve is positioned at a higher lift coefficient compared to cruise, which is necessary to lift the 115,158.18 lb takeoff weight (W_{TO} from the runway within the required 6,000 ft distance.

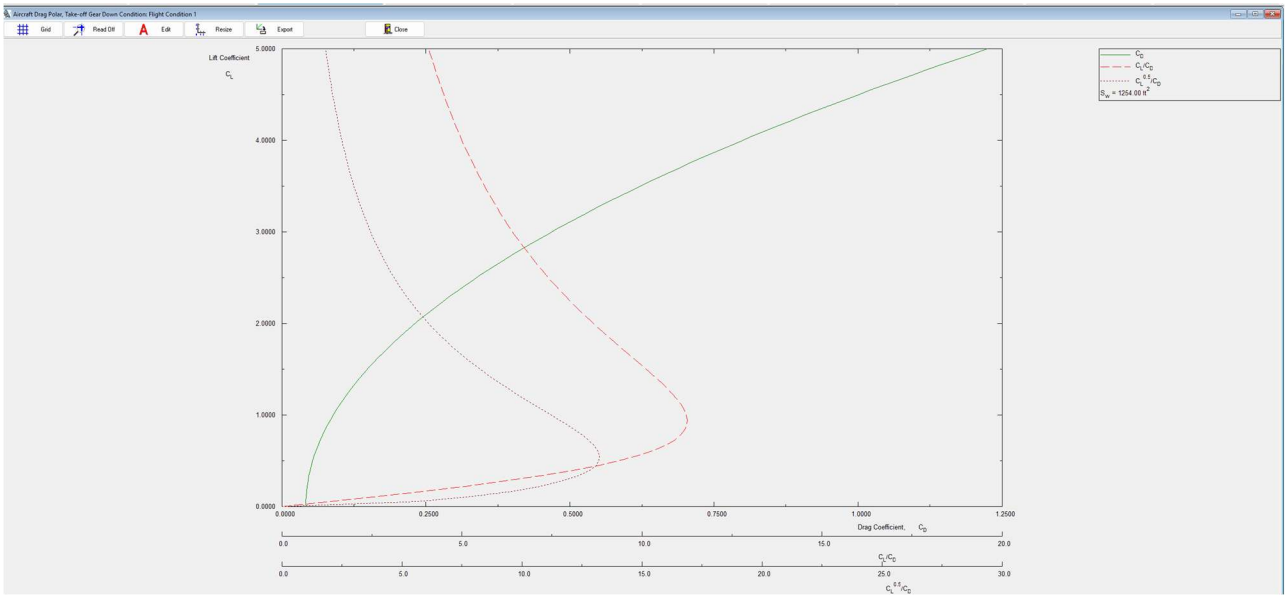

Figure 12: CL Vs CD Takeoff gear down

Once the aircraft reaches its mission altitude, it transitions to the clean configuration (Figure 13). The aircraft is at its most streamlined with all landing gear and flaps retracted, achieving a minimum C_{D0} of 0.0157. In this state, the C_L/C_D curve reaches its highest peak of 18, identifying the optimal lift coefficient needed to achieve the 8,000 NM range efficiently at Mach 0.85 and beyond. Figure 14 shows that the aircraft achieves a maximum cruise speed exceeding Mach 0.85, reaching approximately Mach 0.924, thereby meeting the tradable cruise speed requirement

specified in the RFP. Simultaneously, the $C_L^{0.5}/C_D$ curve peaks at a lower lift coefficient, reflecting the design's optimization for high-speed, long-distance performance.

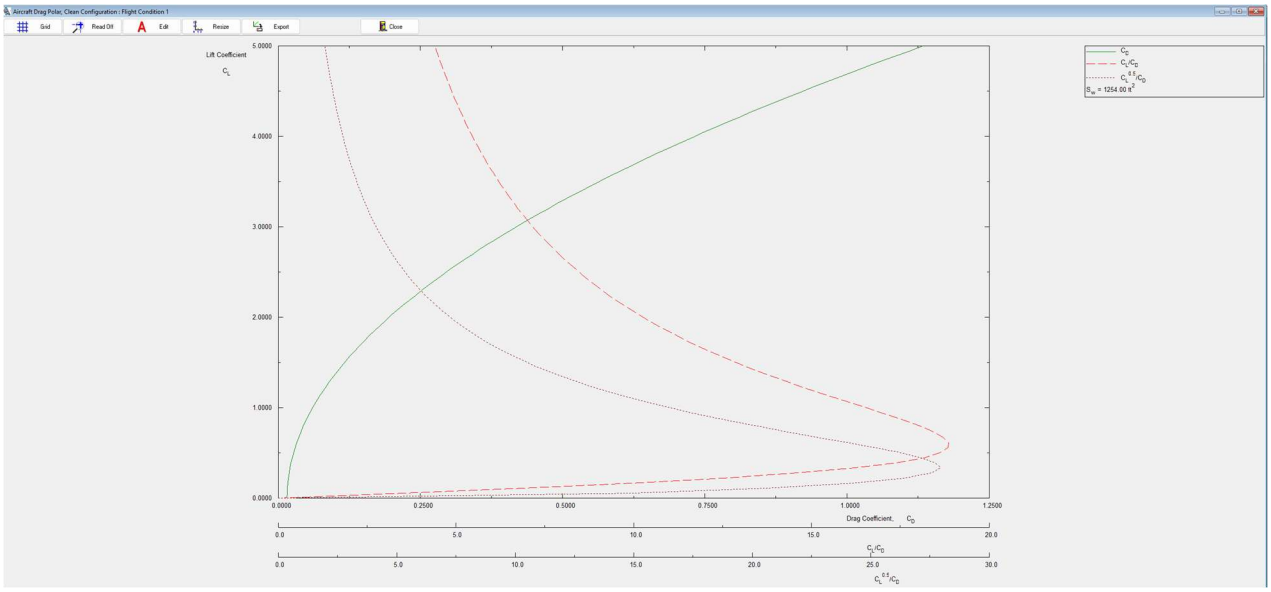

Figure 13: C_L VS C_L clean

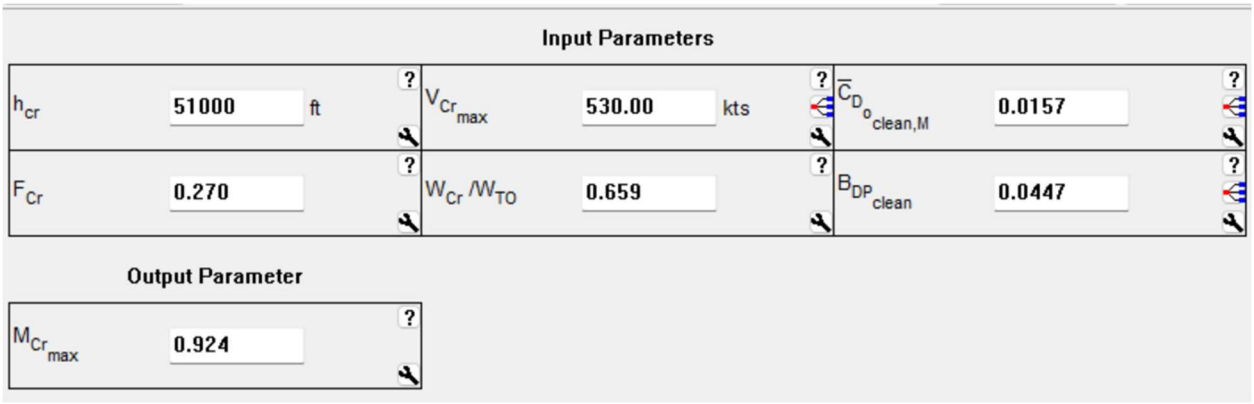

Figure 14: AAA's output for maximum cruise speed

Finally, the landing state (Figure 15) represents the aircraft at its highest drag state, with the C_{D0} rising to 0.1037. The peaks of both the C_L/C_D and $C_L^{0.5}/C_D$ curves are significantly lower and pushed toward much higher lift coefficients. This shift shows that by moving these efficiency peaks, the design ensures the aircraft can maintain stable, controlled flight at the low approach speeds required for a safe touchdown. The increase in drag effectively acts as an aerodynamic brake, ensuring the aircraft can satisfy the mandatory 6,000 ft landing distance requirement.

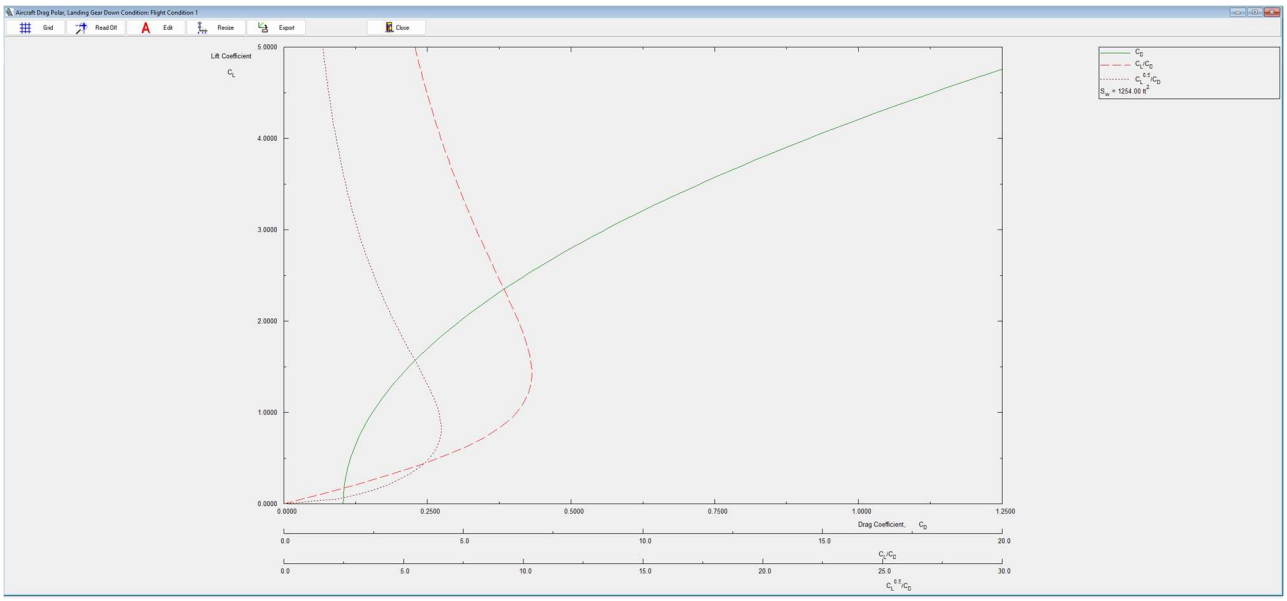

Figure 15: C_L vs C_D Landing, gear down

3.3. Matching plot showing stall speed, takeoff distance, climb, cruise speed & landing distance

The synthesis of these aerodynamic results and the RFP requirements is showcased in the Performance Matching Plot (Figure 16). This plot overlays critical constraints, including stall speed, takeoff distance, and climb gradients, to identify a valid design space where all the criteria are satisfied. By evaluating the intersection of these constraints as shown in Figure 16, the final design point for the aircraft was selected with a Wing Loading ($(W/S)_{TO}$) of 74.58 lb/ft^2 and a Thrust-to-Weight ratio ($(T/W)_{TO}$) of 0.24.

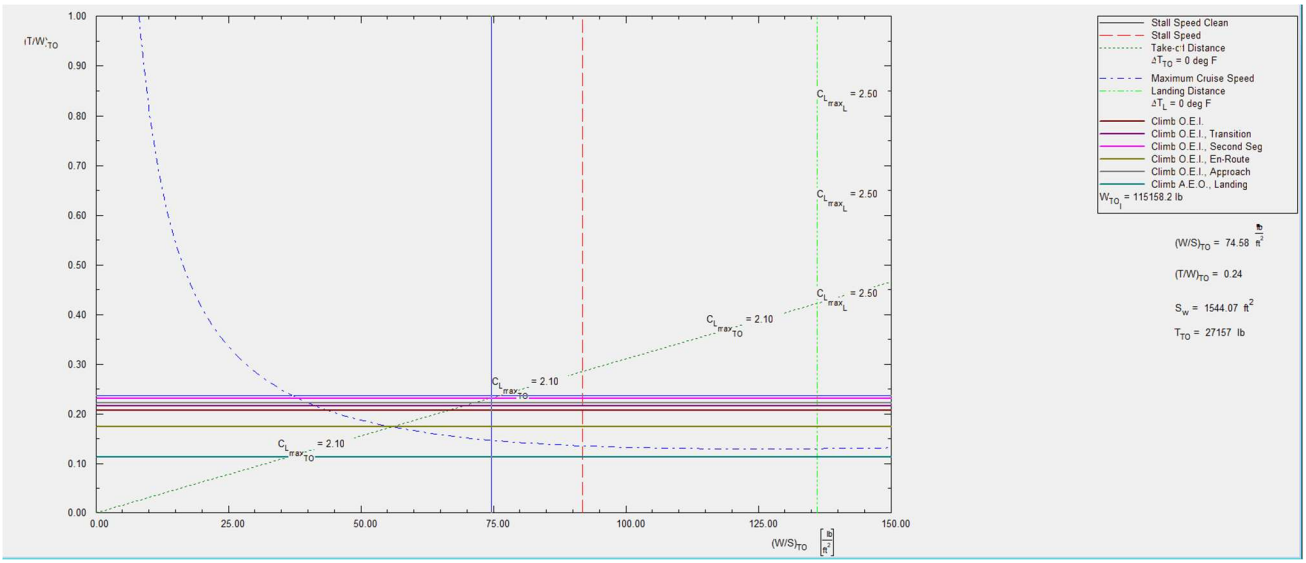

Figure 16: Performance matching plot

This specific design point ensures the aircraft has the appropriate balance of wing area and engine power to safely meet the stall speed requirements and climb gradients required while carrying the 48,049 lb of fuel necessary for the intercontinental mission. The design point was selected graphically from the constraint diagram as a trade-off solution near the intersection of the limiting constraints, balancing low takeoff thrust-to-weight ratio with high wing loading.

3.4. Final W/S and W/P for the RFP aircraft

The final values for W/S and T/W can be found the Table 8 below.

Table 8: Final W/S and T/W for our aircraft

Ratio	AAA calculated value	Design point value
W/S at stall at takeoff weight including flaps	$91.81\frac{lb}{ft^2}$	Not shown
W/S at stall at takeoff weight clean	$91.82\frac{lb}{ft^2}$	$74.58\frac{lb}{ft^2}$
W/S at landing	$107.99\frac{lb}{ft^2}$	Not shown
T/W at takeoff	0.23	0.24

CONCLUSION

In conclusion, the preliminary weight and performance sizing conducted for this project has established a foundation for the aircraft design. By utilizing Advanced Aircraft Analysis (AAA) V5.1 to execute an iterative methodology, the mission requirements defined in the RFP were successfully translated into fundamental mass properties, including a finalized Maximum Take-off Weight (W_{TO}) and Empty Weight (W_E). The integration of Breguet's equations for fuel fraction analysis and historical regression data ensured that the design is both efficient and grounded in industry standards. Furthermore, the sensitivity studies and performance matching plots confirmed that the chosen design point satisfies all critical constraints, such as climb gradients and field length requirements. These results provide the necessary validation to proceed with the detailed configuration design, aerodynamic optimization, and structural layout phases of the aircraft development process.

REFERENCES

[1] McGill University, F. o. (2026). Request for Proposals: Ultra Premium, Long Range Business Jet. Institute for Aerospace Engineering.

[2] Roskam, D. J. (1997). Airplane Design: Part 1 Preliminary Sizing of Airplanes. DARcorporation,.

[3] Ramesh, L., Mugendiran, V., & Sivaraj, G. (2024). Increasing L/D Ratio of Wing by Delaying Flow Separation for Better Aerodynamic Performance. Journal of Applied Fluid Mechanics, 17(12), 2720–2733.

[4] Gulfstream Aerospace, G650 Aircraft Specifications, Gulfstream Aerospace Corporation.

[5] Aviation International News, G650 Wing Data, AIN Media Group.

[6] Aspect Ratio Computed from Published Aircraft Geometry.

[7] Gulfstream Aerospace, G700 Aircraft Specifications, Gulfstream Aerospace Corporation.

[8] Bombardier, Global 7500 Technical Data, Bombardier Aerospace.

[9] Bombardier, Global Express and Global 6000 Specifications, Bombardier Aerospace.

[10] Textron Aviation, Citation X+ Specifications, Textron Aviation Inc.

[11] Federal Aviation Administration, Cessna Citation X Type Certificate Data Sheet, U.S. Department of Transportation.

[12] Dassault Aviation, Falcon 8X Technical Characteristics, Dassault Aviation.

[13] Gulfstream Aerospace, G550 Aircraft Specifications, Gulfstream Aerospace Corporation.

CONTRIBUTIONS

- Milka Ininahazwe
    - Aerodynamic and propulsion efficiency (SFC, L/D) Assumptions, Assumptions in $C_{L_{max}}$ in Takeoff, landing and clean configurations, Plots Matching plot showing stall speed, takeoff distance, climb, cruise speed & landing distance
- Iris Sam Chacko
    - Abstract Presentations, Introduction to weight sizing and performance sizing, Formatting, Aligning, Final Design weights, Sensitivity studiesOswald's efficiency, Drag polar section, Conclusion
- Evelyne Jewitt-Dyck
    - Delta CD0 for flaps and gear section, Matching plot showing stall speed, TO distance, climb, cruise speed & landing distance, Final W/S and W/P for the RFP aircraft section.
- Maverick Hoziel
    - All the AAA software calculations & parameters, RFP summary section, Mission Profile section, Assumptions on SFC, L/D section, Regression line constants (a&b) section, Sensitivity Table section, Interpretation of Sensitivities section, Equivalent Skin Friction Coefficient section, Regression line constants (a&b) for "f vs Swet" plot section, Regression line constants (c&d) for "WTO vs Swet" plot section, Assumptions on Oswald's efficiency factor for TO, L and clean section, Delta CD0 for flaps and gear section, Assumptions in CL max in TO, landing and clean configuration section, Matching plot showing stall speed, TO distance, climb, cruise speed & landing distance section, Final W/S and W/P for the RFP aircraft section.